Supplement of The Cryosphere, 19, 5175–5199, 2025 https://doi.org/10.5194/tc-19-5175-2025-supplement © Author(s) 2025. CC BY 4.0 License.





## Supplement of

## On the statistical relationship between sea ice freeboard and C-band microwave backscatter – a case study with Sentinel-1 and Operation IceBridge

Siqi Liu et al.

Correspondence to: Shiming Xu (xusm@tsinghua.edu.cn)

The copyright of individual parts of the supplement might differ from the article licence.

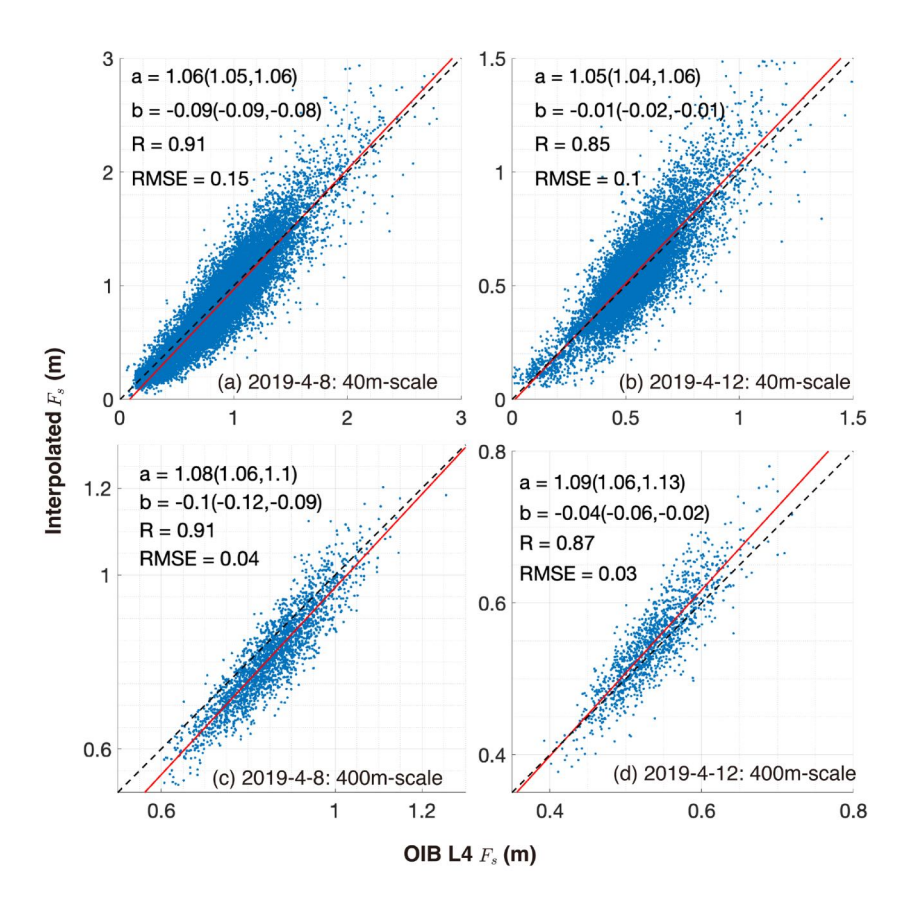


Figure S1: Consistency of the interpolated  $F_s$  and the Operation IceBridge (OIB) standard Level 4 product. The 40m coarsened  $F_s$  based on the 1m-scale  $F_s$  map is compared with the standard OIB product (top row) for both days: April 8th (left column) and April 12th (right column). The along-track 10-footprint mean  $F_s$  comparison for both days is shown in the second row.

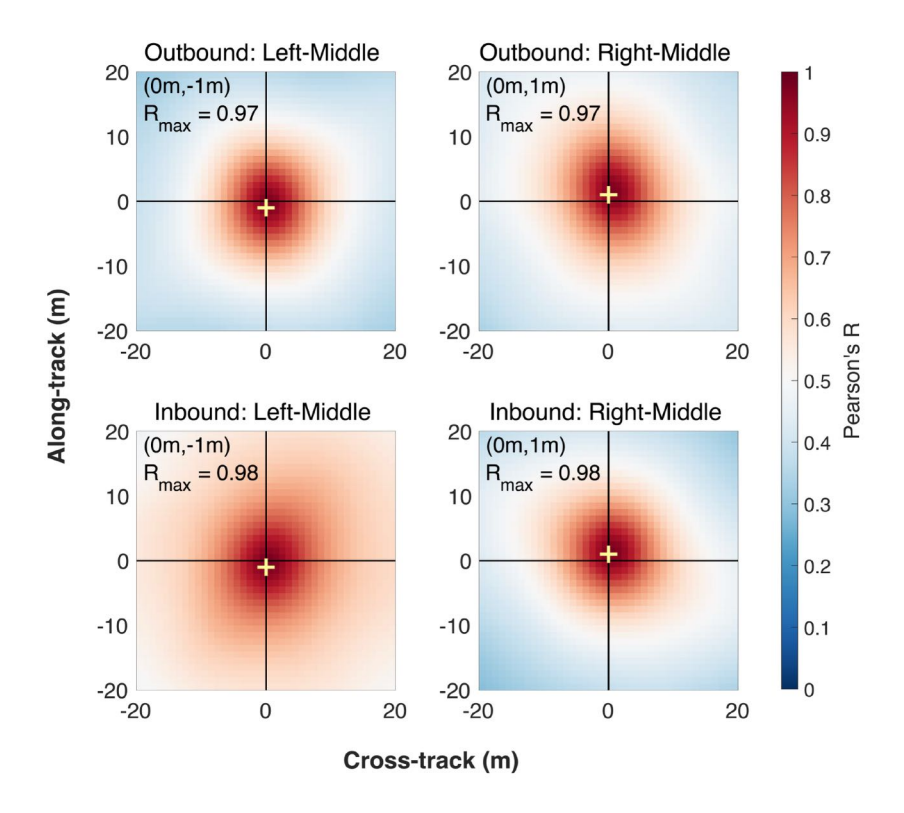


Figure S2: Correlation maps of  $F_s$  (1*m*-scale) between different OIB passes for the outbound (top row) and the inbound (bottom row) sample segment on April 8th, 2019 (see also Fig. 2).

Table S1: Quantitative comparison of statistical relationships with previous studies by Macdonald et al. (2024) and Kortum et al. (2024).

R	40m Fs VS 40m backscatter			100m Fs VS 100m backscatter		
	Macdonald et al. 2024	This study		Kortum et	This study	
		April 8	April 12	al. 2024	April 8	April 12
HH	\	0.48	0.40	0.49	0.58	0.47
HH(FYI)	0.37	0.53	0.44	0.18	0.63	0.50
HH(MYI)	0.48	0.40	0.24	0.34	0.49	0.30
HV	\	0.49	0.47	0.62	0.58	0.59
HV(FYI)	0.40	0.53	0.50	0.32	0.62	0.60
HV(MYI)	0.49	0.41	0.37	0.49	0.50	0.48

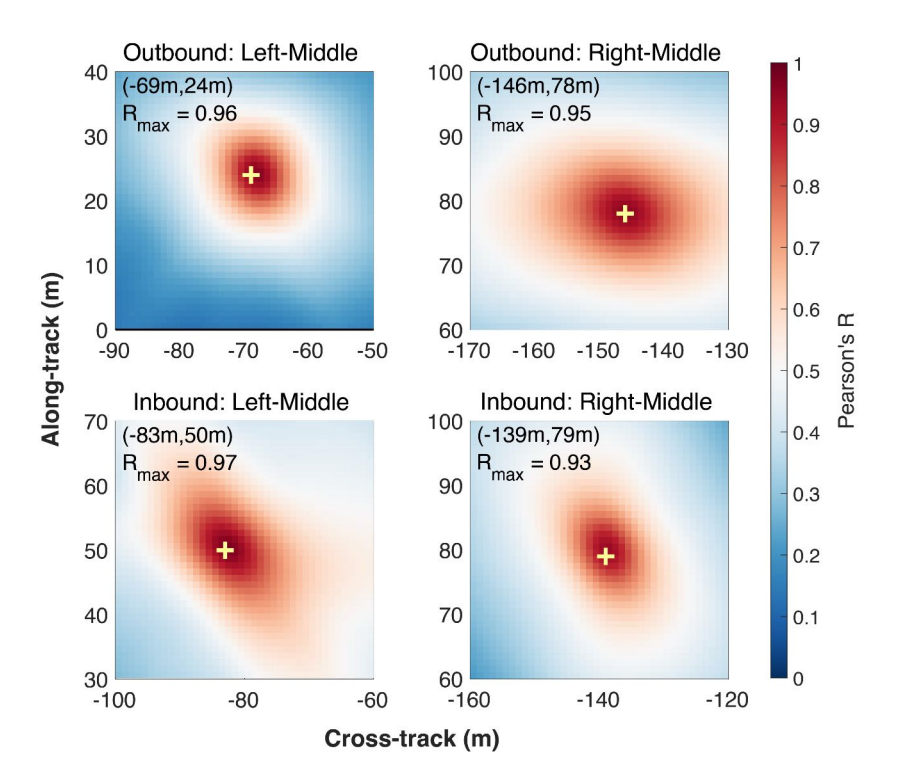


Figure S3: Same as Fig. S2, but for the sample segment on April 12th, 2019 (see also Fig. 3).

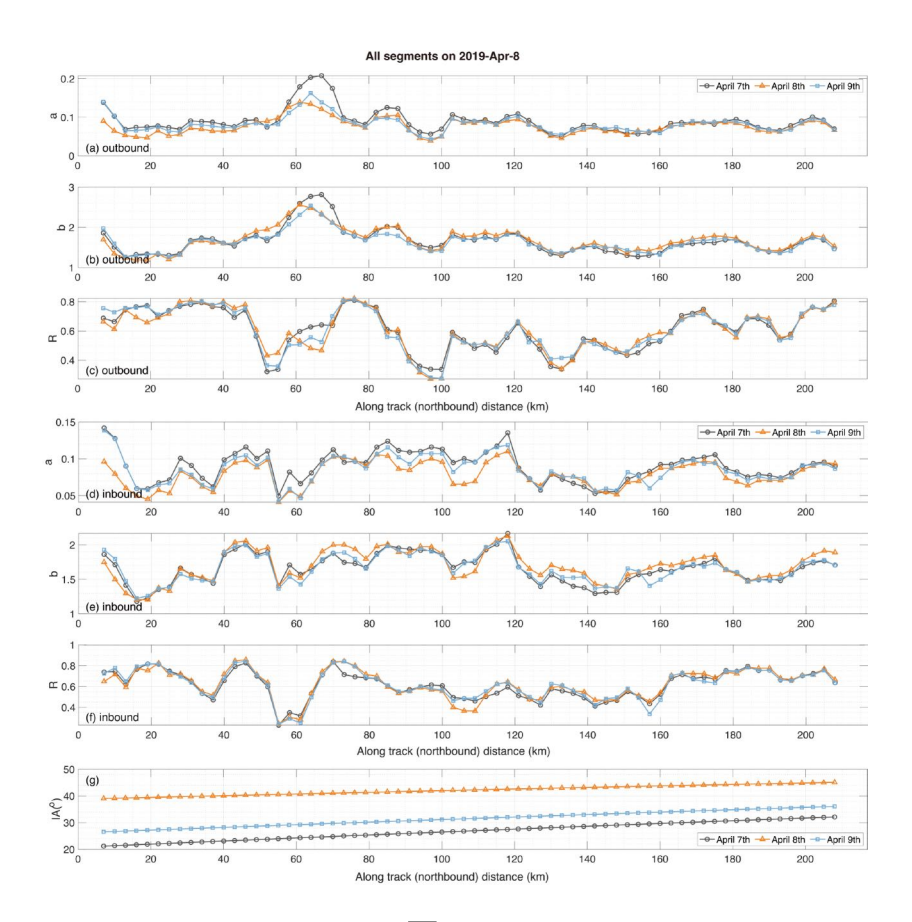


Figure S4: The linear regression  $(\overline{F_s}=a\cdot\sigma_0+b)$  are established using the 200m-scale OIB  $F_s$  and 40m-scale  $\sigma_0$  for all segments on April 8th (panels a-f). The  $\sigma_0$  data were derived from three Sentinel-1 images acquired on April 7th, 8th, and 9th. The corresponding IA variations along the whole OIB track on April 8th are shown in panel g.

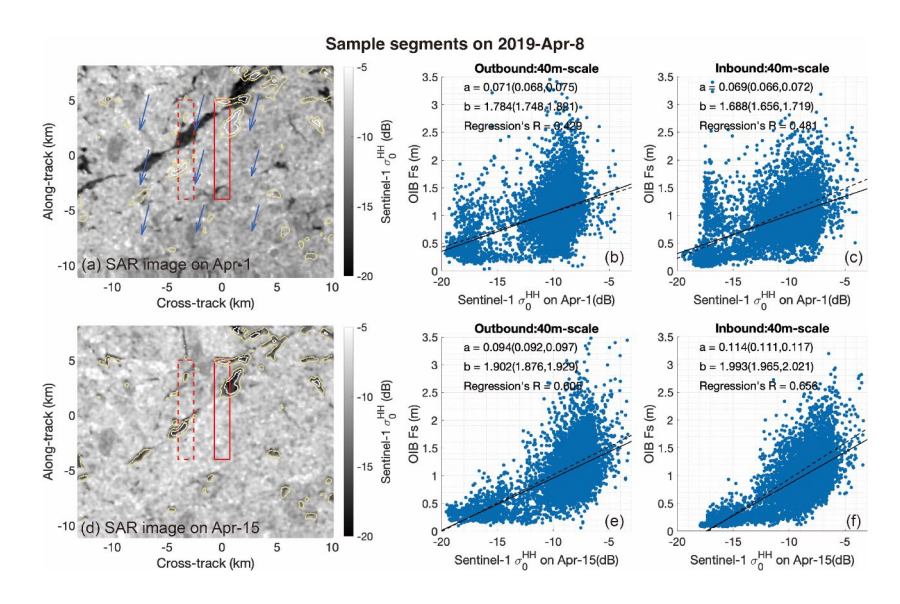


Figure S5: Collocation between the  $F_s$  map for the sample segment on April 8th and the Sentinel-1 maps  $(\sigma_0^{HH})$  from April 1st (top row) and April 12th (second row).

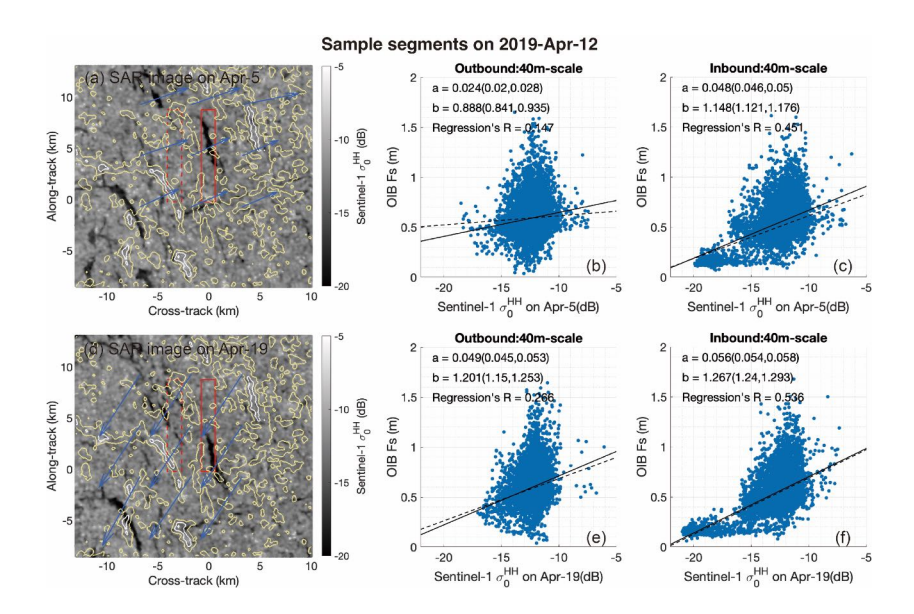


Figure S6: Collocation between the  $F_s$  map for the sample segment on April 12th and the Sentinel-1 maps  $(\sigma_0^{HH})$  from April 5th (top row) and April 19th (second row).

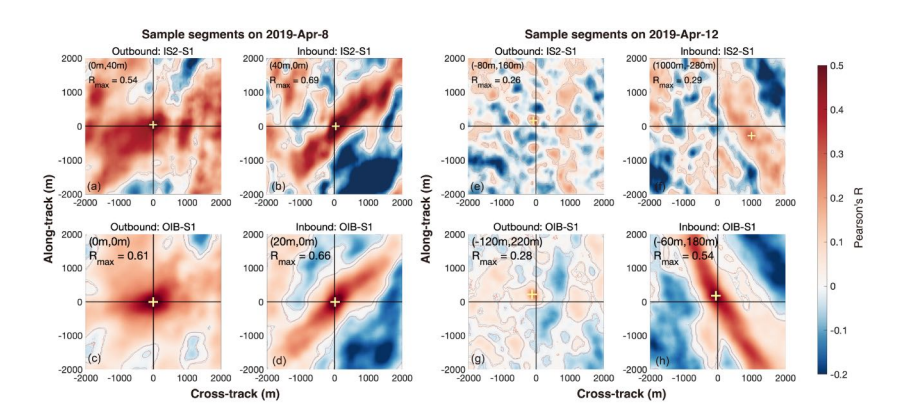


Figure S7: Correlation maps of  $F_s$  on IS2 strong and weak beam segments and Sentinel-1 backscatter (HH channel) for the sample segment on April 8th (left panels) and 12th (right panels). The correlation maps in Fig. 2 and 3 are also shown in the lower row for comparison.

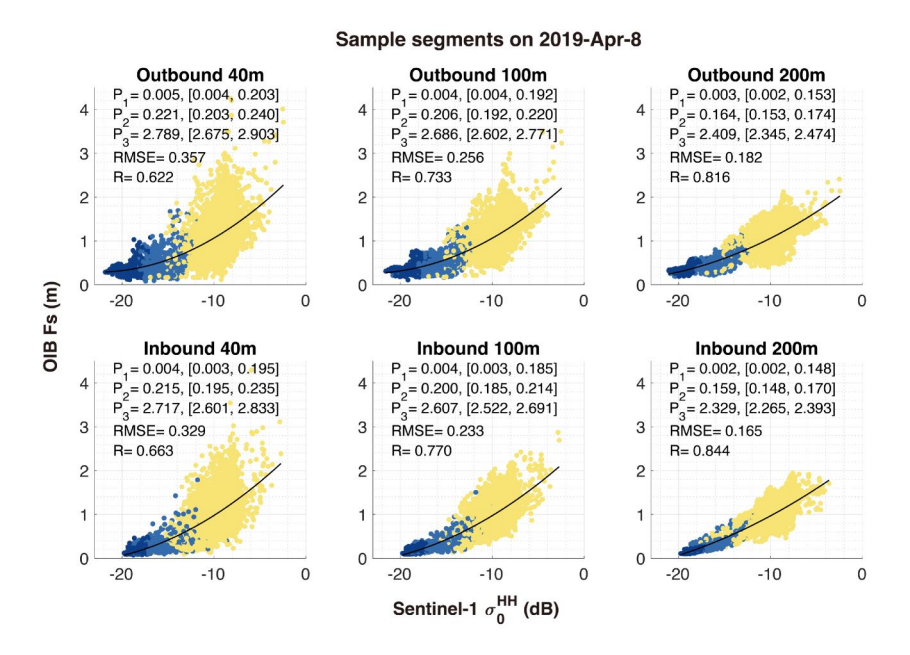


Figure S8: The second-order polynomial regression and scatter plot of the relationship between  $F_s$  and the HH backscatter ( $\sigma_0$ ) for the sample segment on April 8th, 2019. Same as in Fig. 2, three spatial scales of  $F_s$  are used to match the 40*m*-resolution  $\sigma_0$  product: 40*m* (left column), 100*m* (middle column), and 200*m* (right column).

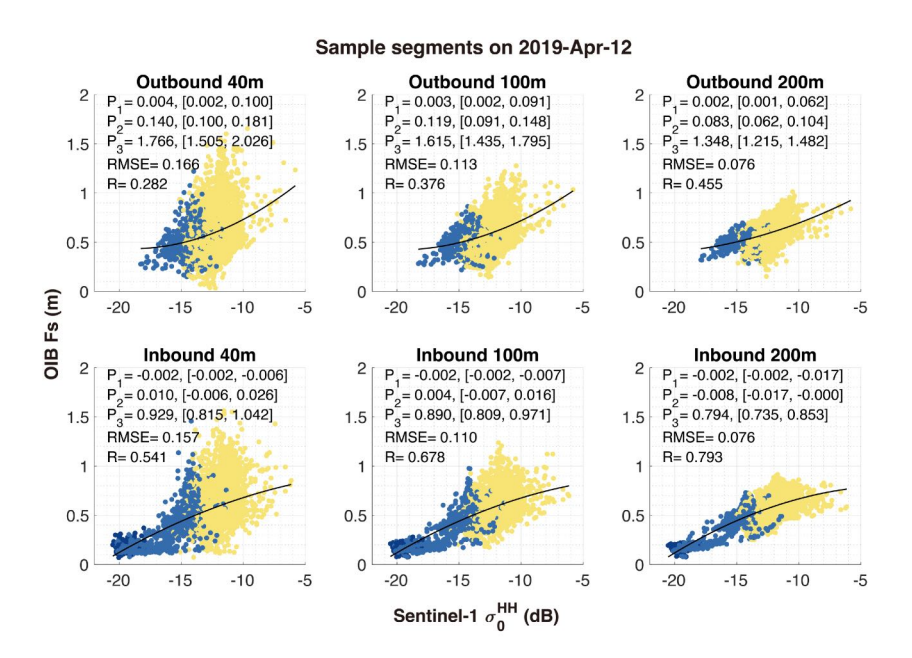


Figure S9: Same as Fig. S8, but for the sample segment on April 12th, 2019.

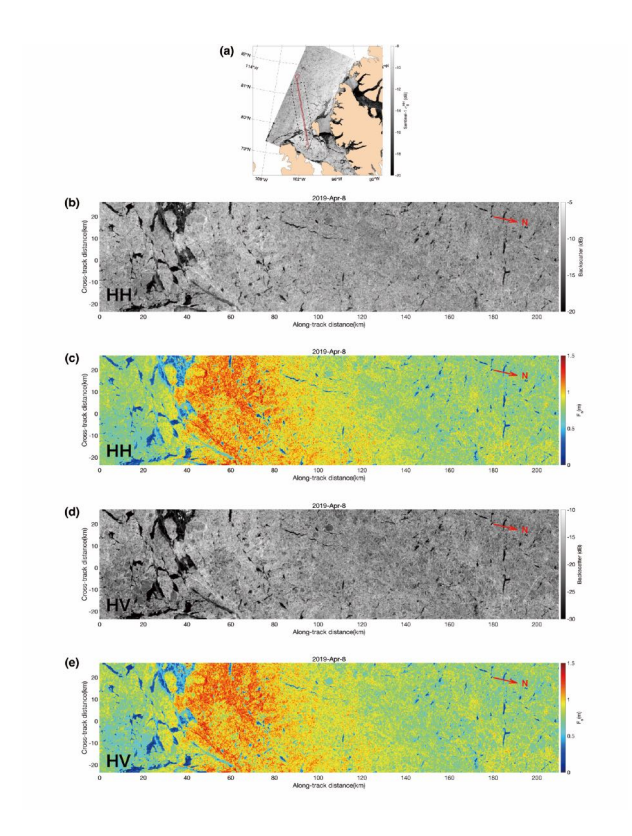


Figure S10: Prediction of freeboard maps for the whole OIB Track on April 8, 2019: The prediction region (dashed black box in panel a), detailed  $\sigma_0$  maps (panels b and d), and corresponding predicted freeboard maps (panels c and e).

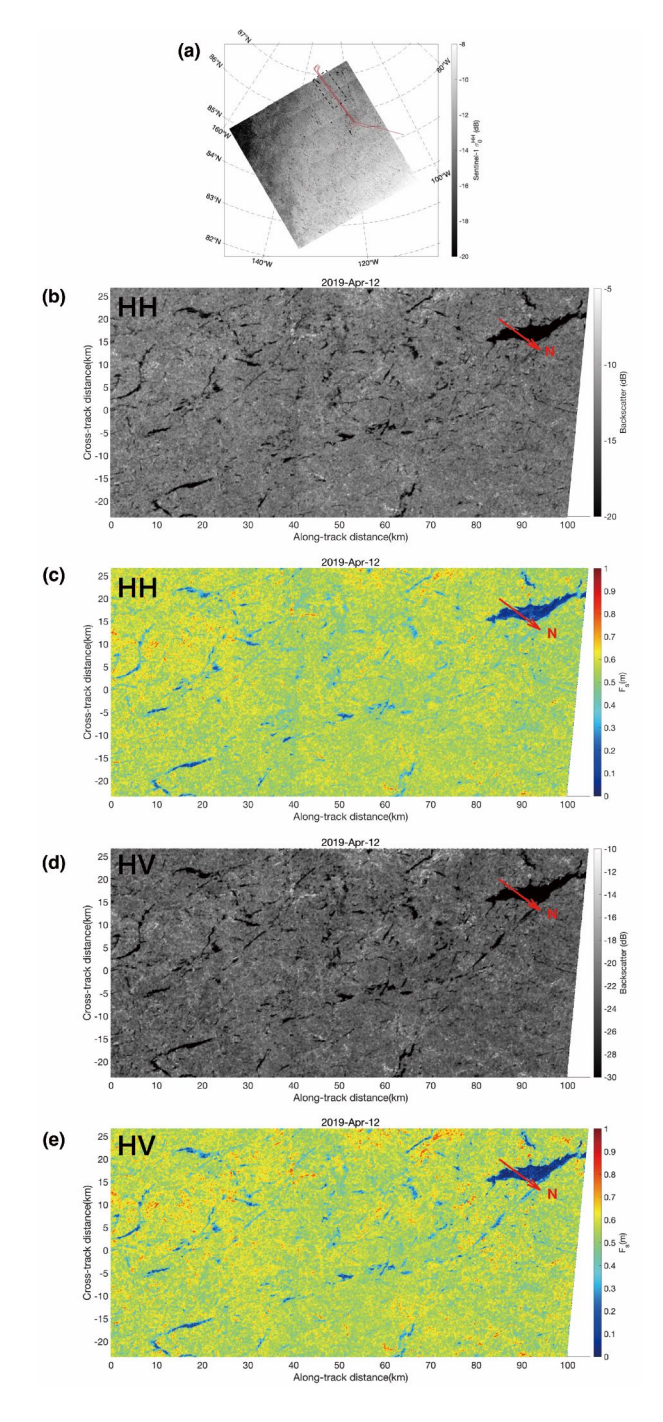


Figure S11: Same as Fig. S10, but for the sample segment on April 12th, 2019.